J. S. Afr. Inst. Min. Metall., vol. 93, no. 10.
Oct. 1993. pp. 253–266.

Effect of depth, span, stope support, and discontinuity strength on the stress and stiffness characteristics of the fractured rock around a tabular mining excavation

by H.A.D. Kirsten* and G.C. Howell*

SYNOPSIS

The mining-induced effects around narrow tabular stopes have traditionally been evaluated in terms of elastic continuum analyses. An understanding of the phenomenological behaviour of the rock surrounding deep-level gold mines has accordingly been developed on the basis of such analyses. However, elastic analyses do not afford reliable representations of the behaviour of rock in which failure may occur on discontinuities. This paper describes investigations that show how the stress and stiffness characteristics of a rockmass are affected under such circumstances for representative ranges of values for the relevant parameters (depth, span, support stiffness, field stress ratio, and discontinuity strength). These investigations afford a substantially different understanding of the mechanical behaviour of rock that is subject to failure. Instead of forming an arch across the abutments, the rock in the hangingwall bears directly across the stope onto the footwall and, instead of being subjected to tension, the nether hangingwall is clamped in compression in the horizontal direction.

SAMEVATTING

Die mynbougeïnduseerde uitwerkings om smal tafelvormige afbouplekke is tradisioneel in terme van elastiese kontinuumontledings geëvalueer. 'n Begrip van die fenomenologiese gedrag van die rots om diepgoudmyne is gevolglik aan die hand van sulke ontledings ontwikkel. Elastiese ontledings gee egter nie betroubare voorstellings van die gedrag van rots waarin swigting op diskontinuïteite kan voorkom nie. Hierdie referaat beskryf ondersoeke wat toon hoe die spannings- en styfheidskenmerke van 'n rotsmassa onder sulke omstandighede vir 'n verteenwoordigende strek van waardes vir die toepaslike parameters (diepte, span styfheid van die stutte, veldspanningsverhouding en diskontinuïteitsterkte) geraak word. Hierdie ondersoeke gee 'n heeltemal ander insig in die meganiese gedrag van rots wat aan swigting onderhewig is. In plaas van 'n boog oor die steunstukke te vorm rus die rots in die dak regstreeks oor die afbouplek op die vloer, en in plaas daarvan dat dit aan trekspanning onderwerp word, word die onderkant van die dak onder drukspanning in die horisontale rigting vasgeklamp.

INTRODUCTION

It was assumed in the past that only stiff fills would effectively limit stope convergence and the associated mining-induced energy release. It was considered that the stability of the stope and the safety of the working place would be enhanced by a reduction in seismic activity and the concomitant rockbursts.

However, stiff fills have not been used extensively in practical applications in this regard because the associated costs are exorbitant. The advantages from the use of backfill could also not be ascribed to its stiffness. The elapsed time in such applications was insufficient for the fill to significantly affect convergence in the back area.

During the past five to ten years, relatively compressible fills have been observed in trial applications to ensure relatively competent conditions close to the working face when placed extensively across the stope and close to the face, and when not allowed to shrink significantly from the hangingwall. These observations are somewhat surprising in view of the originally expected imperative need for fills of substantial stiffness. The complex mechanical behaviour of the partly broken rock around a deep-level stope was evidently not understood.

Kirsten and Stacey[1] postulated a variety of mechanisms for the behaviour of broken rock and for the interaction between broken rock and fill that would explain the observed improvements in stoping conditions associated with the controlled placement of relatively compressible fills. These mechanisms were identified with the kinematic indeterminacy of the rock, which is intrinsic to structural systems in which failure is allowed. According to Desai and Siriwardane[2], the axiom of admissibility is not satisfied in such systems.

The recognition of this phenomenon has enabled the mechanical behaviour of broken rock around a deep-level stope subject to seismic activity and rockbursting to be explained quantitatively. The initial results in this regard were presented by Kirsten and Stacey[3] for a tabular stope spanning 80 m at a depth of 2000 m in a field in which the primitive lateral and vertical stresses were in the proportion 0,25. In particular, the sensitivity of kinematic indeterminacy to type of stope support and discontinuity strength was investigated.

The object of this paper is to extend the preceding investigation to different depth:span proportions and primitive field stress ratios, and to examine the sensitivity of the

* Steffen, Robertson and Kirsten, P.O. Box 55291, Northlands, 2116 Transvaal.
 SA ISSN 0038–223X/3.00 + 0.00. Paper submitted April, 1993; revised paper received July, 1993.

stresses and displacements at key localities around the stope to variations in these parameters. The mining and filling operations were simulated as single steps in this work, as in previously reported studies.

The effect and significance of kinematic indeterminacy in numerically simulated mining configurations have been studied over a period of time. These studies are reviewed here in the next section as they are understood at present to affect the mining problem. This is followed in separate sections by brief presentations of the finite-element solution scheme employed, the model boundary conditions adopted, and the properties of the rockmass, discontinuities, and backfill that were simulated. The accuracy of the results is then evaluated, the results presented, and the findings enumerated in appropriate detail. The salient implications of the proposed postulates with regard to practical mine planning and design are then summarized and verified in conclusion in terms of the field measurements of stresses and displacements reported by others for comparable situations.

DISCONTINUOUS ROCKMASS BEHAVIOUR AND KINEMATIC INDETERMINACY

The rockmass surrounding a tabular stope at depth represents a structural system in which domains of significant extent may be subject to uncontrollably large displacements, depending on the type and extent of failure on discontinuities. The complexities to which this gives rise in numerical analyses depend on the relative strength of the discontinuities and the extent of the failure.

Appropriate solution schemes are required to deal with these complexities, which in turn require that the extent to which failure may occur be known beforehand. This depends upon the innate strength of the discontinuities and on the stresses to which they may be subjected. As a result, the associated computational complexities are also affected by the size and depth of the excavation, the primitive field stress ratio, and the stiffness characteristics of the stope support. Discontinuity strength and field stress ratio affect the problem most. However, in practical applications very little reliable information is usually known about these parameters and, as a result, appropriate ranges of values have to be considered.

An understanding of the extent to which discontinuities may fail and the determination of appropriate ranges of values for the constitutive parameters can be facilitated through a systematic arrangement of the behaviour of the rockmass in terms of kinematic indeterminacy, as shown in Table I.

The stability of the rockmass around the excavation depends upon the magnitude and time-dependent nature of mining-induced displacements. Provision is made in the table for each of four conditions of discontinuity strength and types of stope support. These broadly represent typical categories in which such conditions may be encountered in practice.

Table I

Influence of stope-support reaction and discontinuity condition on equilibrium and seismicity

<table>
<tr><td rowspan="3">Type of Material</td><td rowspan="3">Condition of discontinuity bridges</td><td rowspan="3">Kinematic / displacement freedom</td><td colspan="4">Type of stope support</td><td rowspan="3">Span:depth proportion</td></tr>
<tr><td>No support</td><td>Conventional matpacks and pipesticks</td><td>Deslimed tailings backfill</td><td>Aggregate added backfill</td></tr>
<tr><td colspan="4">Stope-support reaction
Decreasing ◄——————► Increasing</td></tr>
<tr><td>Elastic continuum</td><td>Intact</td><td>Determinate</td><td colspan="4">Stable equilibrium; no ubiquitous seismicity; isolated (low frequency) energy releases (seismicity) of major amplitude may occur in non-homogeneous ground.</td><td>Various</td></tr>
<tr><td rowspan="4">Non-elastic discontinuum</td><td>Failed partly</td><td>Determinate</td><td colspan="4">Stable equilibrium; ubiquitous seismicity belatedly follows face advance at relatively high frequency and low amplitude in homogeneous ground; isolated (low frequency) energy releases (seismicity) of major amplitude may occur in non-homogeneous ground.</td><td>Various</td></tr>
<tr><td rowspan="2">Failing continually (intermediate condition unlikely in practice)</td><td rowspan="2">Indeterminate</td><td>Neutral or unstable equilibrium</td><td colspan="3">Stable equilibrium</td><td rowspan="2">Various</td></tr>
<tr><td colspan="4">Seismicity as either above or below</td></tr>
<tr><td>Failed completely</td><td>Indeterminate</td><td>Unstable equilibrium</td><td colspan="3">Stable equilibrium</td><td rowspan="2">Various</td></tr>
<tr><td colspan="4">Ubiquitous seismicity immediately follows face advance at relatively low frequency and low amplitude in homogeneous ground; isolated (low frequency) energy releases (seismicity) of major amplitude may occur in non-homogeneous ground.</td></tr>
<tr><td colspan="3">Field stress ratio</td><td>Various</td><td>Various</td><td>Various</td><td>Various</td><td></td></tr>
</table>

The static effect of stope support only is considered in Table I. The dynamic support reaction afforded by hydraulic props is accordingly not considered. Furthermore, the occurrence of seismicity in relation to blasting is not specifically accounted for in the table.

As far as discontinuity strength is concerned, provision is made in the first instance for perfectly elastic rock in which no discontinuities occur. In that case, the mining-induced displacements would instantaneously follow advances of the face, and would not be indeterminate or uncontrollably large. In the second instance, provision is made for partly failed discontinuities of such strength that, although the mining-induced displacements would be larger than for elastic rock, they would come to rest soon after advances of the face cease and, as such, would be determinate or limited in magnitude.

In the last instance, along the bottom of Table I, provision is made for discontinuities that have failed completely or, at least, are so weak that advances of the face, unless sufficiently and timeously supported, are followed immediately by uncontrollably large or indeterminate displacements of the rockmass. As an intermediate situation, provision is made in the penultimate instance for discontinuities that are sufficiently weak for the mining-induced displacements to creep with time but yet not to become uncontrollably large.

It has been found, for configurations that are in principle subject to indeterminate displacements, that numerical solutions based on finite-element formulations do not converge because conservation of momentum is not assured. Similarly, nodal perturbations have been found in numerical solution schemes based on finite difference not to decelerate under such conditions.

The potential damage to the excavation under these various conditions of discontinuity strength and the concomitant rockmass stability depend entirely on the time of installation, and the intensity, integrity, and stiffness of the stope support. The effect on each category of behaviour of the specific size and depth of excavation and the specific primitive stress ratio can be taken into consideration as indicated in Table I.

FINITE-ELEMENT SOLUTION SCHEME

The material in the solution scheme adopted comprises an equivalent continuum in which the effects of discontinuities with regard to failure are accounted for, but the discontinuities themselves are not actually modelled[4,5]. The shearing and tensile stresses on planes of specified orientation and ubiquitous presence are limited to specific values over specific proportions of the planes. Dilatation is also allowed along the discontinuities to specified limits. Excessive shearing and tensile stresses are redistributed to unfailed areas elsewhere. Small-strain theory applies to intermediate iterative steps in which stresses and strains are solved in terms of a linear Hooke's law. The strains determined in successive steps are irreversible, and are accumulated over a number of iterations to represent non-elastic behaviour. This process does not allow the simulation of progressive failure. A modified Newton–Raphson over-relaxation routine is employed to accelerate the iteration process.

Only two-dimensional stress states can be simulated in the solution scheme. Quadrilateral or triangular elements can be used, and two sets of joints can be accounted for simultaneously. Although a discontinuity can fail in tension, the development of actual bed separation is not simulated.

The effect of providing for the occurrence and strength of discontinuities as described is that they represent successively alternating jointed and bridged sections along the plane of the discontinuity. The strengths of the jointed sections are prescribed in terms of friction, cohesion, and zero tension, and those of the bridged sections in terms of friction, cohesion, and tension as a fraction of that of the adjoining intact rock.

The shear stiffness of the equivalent continuum depends mainly on the shearing strength and dilatational properties of the discontinuities, and its normal stiffness on that of the intact medium. The equivalent continuum is, as a result, considerably more flexible in shear than is the actual intact material.

BOUNDARY CONDITIONS AND MESH CONFIGURATIONS

The boundaries of the model represent the ground surface 2000 m above the mining horizon, a stationary vertical plane of symmetry through midspan of the stope, a stationary horizontal plane coincident with the centre of the reef horizon, and a vertical plane located remotely from the stope face as given by Kirsten and Stacey[3]. For stope spans of 80 m, this remote vertical boundary is located at 240 m from the vertical plane through midspan and, for spans of 400 m, at 1000 m.

The model is loaded vertically by equal distribution of the weight of every element to the nodes of the element. The remote vertical boundary is subjected to a linearly increasing normal compressive stress that bears a constant proportion to the total vertical gravitational loading. The ground surface is free of stress and unlimited with regard to displacement.

The vertical displacements, determined in the solution scheme, contain the primitive component as a result of the boundary conditions adopted and are therefore not appropriately representative of the displacements induced by mining in the rockmass away from the reef horizon. The displacements calculated on reef in the model are, however, appropriate simulations of the actual displacements induced by mining.

The horizontal displacements obtained from the model are also not appropriate simulations of the actual mining-induced displacements. They also contain the primitive component and cannot be relied upon anywhere in the model.

These limitations do not detract from the appropriateness of the model with regard to its simulation of the effect of backfill or conventional stope support on the distributions of stress in the rockmass, nor on the stope convergence or closure profile of the hangingwall.

The meshes for the depth:span proportions of 2000:80 and 4000:80 were identical, and comprised 1340 nodes and 1311 elements, generally varying in size from 0,5 m at the excavation boundary to 1000 m at the remote boundaries. In the simulation of the greater depth in the second configuration, an equivalent uniformly distributed load was applied along the top horizontal boundary.

The meshes for the 2000:400 and 4000:400 depth:span configurations consisted of 1406 nodes and 1422 elements. As before, the greater depth in the second configuration was simulated by the application of an appropriate uniformly distributed load along the top horizontal boundary. The fill comprised single elements of 1,0 m and, where relevant, were placed within 4 m of the face.

MATERIAL AND STOPE-SUPPORT PROPERTIES SIMULATED

The finite-element analyses that were carried out for various types of support and discontinuity condition are arranged in terms of the postulated classes of behaviour in Table II. All the analyses identified with prefixes A, E, B, and C represent elastic continua. Analyses identified with prefixes F, J, G, and H denote media in which the discontinuity bridges failed partly or, alternatively, in which failure of the bridges terminated. In that condition, the discontinuity bridges still performed a support function. Analyses identified with prefixes T, Q, and R denote media in which the discontinuity bridges failed completely or non-ceasingly and, as a result, were not performing a support function.

Analyses prefixed with A and F represent no support; those with E, J, and T conventional support; those with B, G, and Q deslimed-tailings backfill; and those with C, H, and R aggregate-added backfill. The parameter values for the various analyses are given in Tables III to VI. Specific aspects of the properties of the rockmass, the discontinuities contained in it, and the fill considered can be described as follows.

Rockmass

The intact rock was assumed to have a cohesion of 32 MPa, a friction angle of 50 degrees, an unconfined tensile strength of 20 MPa, a modulus of elasticity of 65 GPa, a Poissons's ratio of 0,2, and a specific weight of 26 kN/m^3. The unconfined compressive strength of the intact rock amounted to 176 MPa in terms of the cohesion and friction angle given.

Discontinuities

Where applicable, the rock was assumed to be intersected by horizontal bedding joints at a spacing of 0,5 m and sub-vertical crossjoints of variable orientation at a spacing of 0,2 m. The friction angle and tensile strength of both joints were assumed to be 35 degrees and zero respectively. The peak cohesion of the cross-joints was taken as 200 kPa, and that for the bedding joints as 200 kPa and 100 kPa for the partially failed and completely failed cases respectively. The residual cohesion for both sets of joints was taken as zero.

As is evident in Tables III to VI, the continuity of the cross-joints was taken as 50 per cent, whereas that of the bedding joints was varied in conjunction with the relative strength of the rock bridges. Target continuities of 75 and 100 per cent were aimed at for the conditions representing partial and complete failure of the rock bridges on the bedding joints in conjunction with relative tensile strengths for the bridges of 0,16 and 0,01 respectively. This objective was generally not achieved or only approximated in the cases of no support or conventional support, which represented relatively small reactive loads on the excavation walls. The problems in this regard were slightly aggravated by a reduction in the primitive field stress ratio. The approach in all these instances was to find the maximum joint continuity in conjunction with the least relative tensile bridge strength that would allow numerical convergence of the solution.

Notwithstanding the variations in the continuity of the bedding joints, the parameters ultimately adopted enable

Table II

Finite-element analyses arranged in terms of stope support and discontinuity bridge condition

Type of material	Condition of discontinuity bridges	Type of stope support: No support	Conventional matpacks and pipesticks	Deslimed-tailings backfill	Aggregate-added backfill	Depth:span
Elastic continuum	Intact	– AA –	EA1 EA2 EA3	BA1 BA2 BA3	– CA –	2000:80
		– AS –	– ES –	– BS –	– CS –	2000:400
		– AB –	– EB –	– BB –	– CB –	4000:80
		– AX –	EX1 EX2 EX3	BX1 BX2 BX3	– CX –	4000:400
	Failed partly	– FA –	JA1 JA2 JA3	GA1 GA2 GA3	– HA –	2000:80
		– FS2 –	JS1 JS2 JS3	GS1 GS2 GS3	– HS2 –	2000:400
		– FB2 –	JB1 JB2 JB3	GB1 GB2 GB3	– HB2 –	4000:80
		– FX2 –	JX1 JX2 JX3	GX1 GX2 GX3	– HX2 –	4000:400
Non-elastic discontinuum	Failing continually	No analyses attempted				– – – –
	Failed completely	No analyses possible	TA1 TA2 TA3	QA1 QA2 QA3	– RA –	2000:80
			TS1 TS2 TS3	QS1 QS2 QS3	– RS2 –	2000:400
			TB1 TB2 TB3	QB1 QB2 QB3	– RB2 –	4000:80
			TX1 TX2 TX3	QX1 QX2 QX3	– RX2 –	4000:400
Field stress ratio, K		0,1 0,25 0,5	0,1 0,25 0,5	0,1 0,25 0,5	0,1 0,25 0,5	

Table III

Values for finite-element model parameters for a depth:span proportion of 2000:80

Parameter	Run identification																						
	AA	EA1	EA2	EA3	BA1	BA2	BA3	CA	FA	JA1	JA2	JA3	GA1	GA2	GA3	HA	TA1	TA2	TA3	QA1	QA2	QA3	RA
Depth, m	2000	2000	2000	2000	2000	2000	2000	2000	2000	2000	2000	2000	2000	2000	2000	2000	2000	2000	2000	2000	2000	2000	2000
Stress ratio	0,25	0,10	0,25	0,50	0,10	0,25	0,50	0,25	0,25	0,10	0,25	0,50	0,10	0,25	0,50	0,25	0,10	0,25	0,50	0,10	0,25	0,50	0,25
Span, m	80	80	80	80	80	80	80	80	80	80	80	80	80	80	80	80	80	80	80	80	80	80	80
Mining/filling step, m	40	40	40	40	40	40	40	40	40	40	40	40	40	40	40	40	40	40	40	40	40	40	40
Bed joints:																							
Incl, °	0	0	0	0	0	0	0	0	0	0	0	0	0	0	0	0	0	0	0	0	0	0	0
Joint cont, %	0	0	0	0	0	0	0	0	75	75	75	75	75	75	75	75	95	100	95	100	100	100	100
Rock brid cont, %	100	100	100	100	100	100	100	100	25	25	25	25	25	25	25	25	5	0	5	0	0	0	0
Peak coh, kPa	200	200	200	200	200	200	200	200	200	200	200	200	200	200	200	200	100	100	100	100	100	100	100
Tens strength, kPa	0	0	0	0	0	0	0	0	0	0	0	0	0	0	0	0	0	0	0	0	0	0	0
Rel brid strength	0,16	0,16	0,16	0,16	0,16	0,16	0,16	0,16	0,16	0,16	0,16	0,16	0,16	0,16	0,16	0,16	0,01	0,01	0,01	0,01	0,01	0,01	0,01
Cross joints:																							
Incl, °	90	90	90	90	90	90	90	90	90	90	90	90	90	90	90	90	90	90	90	90	90	90	90
Joint cont, %	0	0	0	0	0	0	0	0	50	50	50	50	50	50	50	50	50	50	50	50	50	50	50
Rock brid cont, %	100	100	100	100	100	100	100	100	50	50	50	50	50	50	50	50	50	50	50	50	50	50	50
Peak coh, kPa	200	200	200	200	200	200	200	200	200	200	200	200	200	200	200	200	200	200	200	200	200	200	200
Tens strength, kPa	0	0	0	0	0	0	0	0	0	0	0	0	0	0	0	0	0	0	0	0	0	0	0
Rel brid strength	0,16	0,16	0,16	0,16	0,16	0,16	0,16	0,16	0,16	0,16	0,16	0,16	0,16	0,16	0,16	0,16	0,01	0,01	0,01	0,01	0,01	0,01	0,01
Tailings content in fill, %	No fill	No fill	No fill	No fill	100	100	100	0	No fill	No fill	No fill	No fill	100	100	100	0	No fill	No fill	No fill	100	100	100	0
Aggregate content in fill, %	–	–	–	–	0	0	0	100	–	–	–	–	0	0	0	100	–	–	–	0	0	0	100
Backfill parameters:																							
A, MPa	–	–	–	–	3916	3916	3916	6150	–	–	–	–	3916	3916	3916	6150	–	–	–	3916	3916	3916	6150
B	–	–	–	–	0,08	0,08	0,08	0,08	–	–	–	–	0,08	0,08	0,08	0,08	–	–	–	0,08	0,08	0,08	0,08
C	–	–	–	–	3,0	3,0	3,0	3,0	–	–	–	–	3,0	3,0	3,0	3,0	–	–	–	3,0	3,0	3,0	3,0
D, %	–	–	–	–	20	20	20	17	–	–	–	–	20	20	20	17	–	–	–	20	20	20	17
E, MPa	–	–	–	–	489	489	489	1136	–	–	–	–	489	489	489	1136	–	–	–	489	489	489	1136
F	–	–	–	–	0,3	0,3	0,3	0,3	–	–	–	–	0,3	0,3	0,3	0,3	–	–	–	0,3	0,3	0,3	0,3
Const. support pressure, kPa	–	300	300	300	–	–	–	–	3	300	300	300	–	–	–	–	300	300	300	–	–	–	3

Table IV

Values for finite-element model parameters for a depth:span proportion of 2000:400

Parameter	Run identification																		
	AS	BS	CS	ES	FS2	JS1	JS2	JS3	GS1	GS2	GS3	HS2	TS1	TS2	TS3	QS1	QS2	QS3	RS2
Depth, m	2000	2000	2000	2000	2000	2000	2000	2000	2000	2000	2000	2000	2000	2000	2000	2000	2000	2000	2000
Stress ratio	0,25	0,25	0,25	0,25	0,25	0,10	0,25	0,50	0,10	0,25	0,50	0,25	0,10	0,25	0,50	0,10	0,25	0,50	0,25
Span, m	400	400	400	400	400	400	400	400	400	400	400	400	400	400	400	400	400	400	400
Mining/filling step, m	200	200	200	200	200	200	200	200	200	200	200	200	200	200	200	200	200	200	200
Bed joints:																			
Incl, °	0	0	0	0	0	0	0	0	0	0	0	0	0	0	0	0	0	0	0
Joint cont, %	0	0	0	0	30	20	40	40	75	75	75	75	0	0	0	100	100	100	100
Rock brid cont, %	100	100	100	100	70	80	60	60	25	25	25	25	100	100	100	0	0	0	0
Peak coh, kPa	200	200	200	200	200	200	200	200	200	200	200	200	100	100	100	100	100	100	100
Tens strength, kPa	0	0	0	0	0	0	0	0	0	0	0	0	0	0	0	0	0	0	0
Rel brid strength	0,16	0,16	0,16	0,16	0,16	0,16	0,16	0,16	0,16	0,16	0,16	0,16	0,14	0,12	0,12	0,01	0,01	0,01	0,01
Cross joints:																			
Incl, °	90	90	90	90	90	90	90	90	90	90	90	90	90	90	90	90	90	90	90
Joint cont, %	0	0	0	0	50	50	50	50	50	50	50	50	50	50	50	50	50	50	50
Rock brid cont, %	100	100	100	100	50	50	50	50	50	50	50	50	50	50	50	50	50	50	50
Peak coh, kPa	200	200	200	200	200	200	200	200	200	200	200	200	200	200	200	200	200	200	200
Tens strength, kPa	0	0	0	0	0	0	0	0	0	0	0	0	0	0	0	0	0	0	0
Rel brid strength	0,16	0,16	0,16	0,16	0,16	0,16	0,16	0,16	0,16	0,16	0,16	0,16	0,01	0,01	0,01	0,01	0,01	0,01	0,01
Tailings content in fill	No fill	100	0	No fill	No fill	No fill	No fill	No fill	100	100	100	0	No fill	No fill	No fill	100	100	100	0
Aggregate content in fill, %	–	0	100	–	–	–	–	–	0	0	0	100	–	–	–	0	0	0	100
Backfill parameters:																			
A, MPa	–	3916	6125	–	–	–	–	–	3916	3916	3916	6150	–	–	–	3916	3916	3916	6150
B	–	0,08	0,08	–	–	–	–	–	0,08	0,08	0,08	–	–	–	–	0,08	0,08	0,08	0,08
C	–	3,0	3,0	–	–	–	–	–	3,0	3,0	3,0	3,0	–	–	–	3,0	3,0	3,0	3,0
D, %	–	20	17	–	–	–	–	–	20	20	20	17	–	–	–	20	20	20	17
E, MPa	–	489	1136	–	–	–	–	–	489	489	489	1136	–	–	–	489	489	489	1136
F	–	0,3	0,3	–	–	–	–	–	0,3	0,3	0,3	0,3	–	–	–	0,3	0,3	0,3	0,3
Const support pressure, kPa	–	–	–	300	–	300	300	300	–	–	–	–	300	300	300	–	–	–	–

Table V

Values for finite-element model parameters for a depth:span proportion of 4000:80

Parameter	Run identification																		
	AB	EB	BB	CB	FB2	JB1	JB2	JB3	GB1	GB2	GB3	HB2	TB1	TB2	TB3	QB1	QB2	QB3	RB2
Depth, m	4000	4000	4000	4000	4000	4000	4000	4000	4000	4000	4000	4000	4000	4000	4000	4000	4000	4000	4000
Stress ratio	0,25	0,25	0,25	0,25	0,25	0,10	0,25	0,50	0,10	0,25	0,50	0,25	0,10	0,25	0,50	0,10	0,25	0,50	0,25
Span, m	80	80	80	80	80	80	80	80	80	80	80	80	80	80	80	80	80	80	80
Mining/filling step, m	40	40	40	40	40	40	40	40	40	40	40	40	40	40	40	40	40	40	40
Bed joints:																			
Incl, °	0	0	0	0	0	0	0	0	0	0	0	0	0	0	0	0	0	0	0
Joint cont, %	0	0	0	0	75	75	75	75	75	75	75	75	95	95	95	100	100	100	100
Rock brid cont, %	100	100	100	100	25	25	25	25	25	25	25	25	5	5	5	0	0	0	0
Peak coh, kPa	200	200	200	200	200	200	200	200	200	200	200	200	100	100	100	100	100	100	100
Tens strength, kPa	0	0	0	0	0	0	0	0	0	0	0	0	0	0	0	0	0	0	0
Rel brid strength	0,16	0,16	0,16	0,16	0,16	0,16	0,16	0,16	0,16	0,16	0,16	0,16	0,01	0,01	0,01	0,01	0,01	0,01	0,01
Cross joints:																			
Incl, °	90	90	90	90	90	90	90	90	90	90	90	90	90	90	90	90	90	90	90
Joint cont, %	0	0	0	0	50	50	50	50	50	50	50	50	50	50	50	50	50	50	50
Rock brid cont, %	100	100	100	100	50	50	50	50	50	50	50	50	50	50	50	50	50	50	50
Peak coh, kPa	200	200	200	200	200	200	200	200	200	200	200	200	200	200	200	200	200	200	200
Tens strength, kPa	0	0	0	0	0	0	0	0	0	0	0	0	0	0	0	0	0	0	0
Rel brid strength	0,16	0,16	0,16	0,16	0,16	0,16	0,16	0,16	0,16	0,16	0,16	0,16	0,01	0,01	0,01	0,01	0,01	0,01	0,01
Tailings content in fill	No fill	No fill	100	0	No fill	No fill	No fill	No fill	100	100	100	0	No fill	No fill	No fill	100	100	100	0
Aggregate content in fill, %	–	–	0	100	–	–	–	–	0	0	0	100	–	–	–	0	0	0	100
Backfill parameters:																			
A, MPa	–	–	3916	6150	–	–	–	–	3916	3916	3916	6150	–	–	–	3916	3916	3916	6150
B	–	–	0,08	0,08	–	–	–	–	0,08	0,08	0,08	0,08	–	–	–	0,08	0,08	0,08	0,08
C	–	–	3,0	3,0	–	–	–	–	3,0	3,0	3,0	3,0	–	–	–	3,0	3,0	3,0	3,0
D, %	–	–	20	17	–	–	–	–	20	20	20	17	–	–	–	20	20	20	17
E, MPa	–	–	489	1136	–	–	–	–	489	489	489	1136	–	–	–	489	489	489	1136
F	–	–	0,3	0,3	–	–	–	–	0,3	0,3	0,3	0,3	–	–	–	0,3	0,3	0,3	0,3
Const support pressure, kPa	–	300	–	–	–	300	300	300	–	–	–	–	300	300	300	–	–	–	–

Table VI

Values for finite-element model parameters for a depth: Span proportion of 4000:400

Parameter	Run identification																					
	AX	EX1	EX2	EX3	BX1	BX2	BX3	CX	FX2	JX1	JX2	JX3	GX1	GX2	GX3	HX2	TX1	TX2	TX3	QX1	QX2	QX3	RX2
Depth, m	4000	4000	4000	4000	4000	4000	4000	4000	4000	4000	4000	4000	4000	4000	4000	4000	4000	4000	4000	4000	4000	4000	4000
Stress ratio	0,25	0,10	0,25	0,50	0,10	0,25	0,50	0,25	0,25	0,10	0,25	0,50	0,10	0,25	0,50	0,25	0,10	0,25	0,50	0,10	0,25	0,50	0,25
Span, m	400	400	400	400	400	400	400	400	400	400	400	400	400	400	400	400	400	400	400	400	400	400	400
Mining/filling step, m	200	200	200	200	200	200	200	200	200	200	200	200	200	200	200	200	200	200	200	200	200	200	200
Bed joints:																							
Incl, °	0	0	0	0	0	0	0	0	0	0	0	0	0	0	0	0	0	0	0	0	0	0	0
Joint cont, %	0	0	0	0	0	0	0	0	50	10	60	60	75	75	75	75	0	0	0	100	100	100	100
Rock brid cont, %	100	100	100	100	100	100	100	100	50	90	40	40	25	25	25	25	100	100	100	0	0	0	0
Peak coh, kPa	200	200	200	200	200	200	200	200	200	200	200	200	200	200	200	200	100	100	100	100	100	100	100
Tens strength, kPa	0	0	0	0	0	0	0	0	0	0	0	0	0	0	0	0	0	0	0	0	0	0	0
Rel brid strength	0,16	0,16	0,16	0,16	0,16	0,16	0,16	0,16	0,16	0,16	0,16	0,16	0,16	0,16	0,16	0,16	0,14	0,10	0,10	0,01	0,01	0,01	0,01
Cross joints:																							
Incl, °	90	90	90	90	90	90	90	90	90	90	90	90	90	90	90	90	90	90	90	90	90	90	90
Joint cont, %	0	0	0	0	0	0	0	0	50	50	50	50	50	50	50	50	50	50	50	50	50	50	50
Rock brid cont, %	100	100	100	100	100	100	100	100	50	50	50	50	50	50	50	50	50	50	50	50	50	50	50
Peak coh, kPa	200	200	200	200	200	200	200	200	200	200	200	200	200	200	200	200	200	200	200	200	200	200	200
Tens strength, kPa	0	0	0	0	0	0	0	0	0	0	0	0	0	0	0	0	0	0	0	0	0	0	0
Rel brid strength	0,16	0,16	0,16	0,16	0,16	0,16	0,16	0,16	0,16	0,16	0,16	0,16	0,16	0,16	0,16	0,16	0,01	0,01	0,01	0,01	0,01	0,01	0,01
Tailings content in fill, %	No fill	No fill	No fill	No fill	100	100	100	0	No fill	No fill	No fill	No fill	100	100	100	0	No fill	No fill	No fill	100	100	100N	0
Aggregate content in fill, %	–	–	–	–	0	0	0	100	–	–	–	–	0	0	0	100	–	–	–	0	0	0	100
Backfill parameters:																							
A, MPa	–	–	–	–	3916	3916	3916	6150	–	–	–	–	3916	3916	3916	6150	–	–	–	3916	3916	3916	6150
B	–	–	–	–	0,08	0,08	0,08	0,08	–	–	–	–	0,08	0,08	0,08	0,08	–	–	–	0,08	0,08	0,08	0,08
C	–	–	–	–	3,0	3,0	3,0	3,0	–	–	–	–	3,0	3,0	3,0	3,0	–	–	–	3,0	3,0	3,0	3,0
D, %	–	–	–	–	20	20	20	17	–	–	–	–	20	20	20	17	–	–	–	20	20	20	17
E, MPa	–	–	–	–	489	489	489	1136	–	–	–	–	489	489	489	1136	–	–	–	489	489	489	1136
F	–	–	–	–	0,3	0,3	0,3	0,3	–	–	–	–	0,3	0,3	0,3	0,3	–	–	–	0,3	0,3	0,3	0,3
Const. support pressure, kPa	–	300	300	300	–	–	–	–	–	300	300	300	–	–	–	–	300	300	300	–	–	–	–

reliable comparisons to be drawn between the cases representing partially failed and completely failed joints. The numerical difficulties experienced in obtaining convergent solutions for cases corresponding to extremely weak joints and to very light support confirm the sensitivity of the stability or equilibrium condition of the excavation to the displacement freedom of the rockmass, and the significance of the underlying characteristic kinematic indeterminacy.

Fill

The fill was considered to be subject to a constant proportional loading path. The stress–strain relationships for deslimed tailings and aggregate-added fills were respectively considered to be linear for strains, D, in excess of 20 per cent, and 17 per cent with corresponding moduli of elasticity, E, of 489 kPa and 1136 kPa and Poisson's ratios, F, of 0,3 and 0,3. The constitutive equation for strains less than D was assumed to be given by the power law

$$\sigma_1 = A(\varepsilon_1 - B)^C$$

It was further assumed that a stope closure of 7 per cent would occur before the fill would begin to take load. This allowed for the initial closure of the hangingwall, which occurs immediately after mining before the fill is placed or, alternatively, for the shrinkage of the fill prior to the onset of loading. The values for constants A, B, C, D, E, and F are given in Tables III to VI for the various analyses.

ACCURACY OF SOLUTION SCHEME

The hangingwall closures, which were determined by substitution of the rock–fill contact pressures (obtained from the finite-element solutions) in the adopted stress–strain law for the fill, are given in brackets in Table VII alongside the closures that were determined from the numerical solutions.

Likewise, the rock–fill contact pressures, which can be determined by substitution of the hangingwall closures from the numerical solutions in the adopted stress–strain law for the fill, are given in brackets in Table VIII alongside the rock–fill contact pressures, which were determined from the numerical solutions.

Comparisons of the back-figured values for the hangingwall closures and the rock–fill contact pressures with the corresponding values determined from the numerical solutions enable the accuracy of the solution scheme to be evaluated. It can be shown from Tables VII and VIII that the accuracy of the solution scheme with regard to closure is on average 3 per cent, and the accuracy with regard to rock–fill contact pressure is on average 13 per cent. The greater accuracy with regard to closure follows from the fact that the solution scheme is essentially a displacement-solving, rather than a stress-solving, method. An accuracy of 3 per cent with regard to closure is satisfactory in view of the complexities imposed on the numerical solution procedure by discontinuity failure.

It is also evident from Tables VII and VIII that the largest inaccuracies with regard to midspan convergence and support pressure occurred for the 4000:400 depth:span configuration. This was due to the fact that, for this configuration, the percentage strain, to which the closure corresponded, was just larger than that represented by limit D. The discontinuity in the stress–strain law represented by the change-over of functions across this limit was not only unnecessary because it was not exceeded significantly, but was also counter-productive with regard to the efficacy of the numerical solution process. As a result, the stress–strain law for the fill could have been specified by a single power law without any loss in accuracy.

Table VII

Hangingwall closures (mm) at 5,0 m from face and in back area, determined from finite-element analyses for K = 0,25

Type of material	Condition of discontinuity bridges	Type of stope support: No support	Conventional matpacks and pipesticks	Deslimed-tailings backfill	Aggregate-added backfill	Depth:span
Elastic continuum	Intact	32 63	32 62	(53) 32 (64) 62	(55) 32 (66) 62	2000:80
		71 177	71 176	(55) 49 (113) 109	(56) 47 (105) 103	2000:400
		64 126	64 125	(62) 61 (114) 114	(61) 59 (110) 111	4000:80
		142 355	142 354	(78) 75 (165) 147	(72) 69 (134) 129	4000:400
	Failed partly	73 110	72 107	(68) 69 (94) 94	(71) 70 (90) 90	2000:80
		162 409	159 402	(84) 87 (132) 130	(86) 86 (120) 118	2000:400
		147 229	147 228	(109) 108 (139) 140	(104) 106 (130) 127	4000:80
		323 745	329 740	(122) 123 (181) 156	(114) 113 (139) 133	4000:400
Non-elastic discontinuum	Failing continually	No analyses attempted				– – – –
	Failed completely	No analyses possible	80 143	(71) 72 (99) 100	(75) 73 (94) 94	2000:80
			235 486	(91) 87 (134) 133	(88) 88 (121) 121	2000:400
			156 255	(112) 110 (142) 142	(104) 106 (132) 128	4000:80
			486 1061	(122) 123 (182) 157	(112) 112 (140) 133	4000:400
Distance from face, m		5 40/200	5 40/200	5 40/200	5 40/200	

Table VIII

Rock-fill contact loads (m head of rock) 5,0 m from face and in back area, determined from finite-element analyses for $K = 0,25$

Type of material	Condition of discontinuity bridges	Type of stope support: No support	Conventional matpacks and pipesticks	Deslimed-tailings backfill	Aggregate-added backfill	Depth:span
Elastic continuum	Intact	0 0	12 12	(0) 3 (14) 18	(0) 6 (20) 32	2000:80
		0 0	12 12	(2) 4 (482) 387	(1) 7 (544) 439	2000:400
		0 0	12 12	(10) 12 (496) 491	(14) 17 (666) 660	4000:80
		0 0	12 12	(62) 54 (1585) 1722	(55) 51 (1730) 1819	4000:400
Non-elastic discontinuum	Failed partly	0 0	12 12	(31) 27 (193) 193	(53) 58 (239) 238	2000:80
		0 0	12 12	(156) 110 (951) 894	(247) 144 (972) 927	2000:400
		0 0	12 12	(381) 395 (1191) 1166	(534) 502 (1250) 1396	4000:80
		0 0	12 12	(761) 604 (1882) 2554	(814) 667 (1992) 2279	4000:400
	Failing continually	No analyses attempted				– – – –
	Failed completely	No analyses possible	12 12	(39) 35 (254) 250	(66) 78 (300) 297	2000:80
			12 12	(163) 110 (1027) 953	(244) 181 (1028) 983	2000:400
			12 12	(412) 447 (1267) 1262	(554) 543 (1255) 1470	4000:80
			12 12	(758) 603 (1912) 2605	(754) 668 (2036) 2328	4000:400
Distance from face, m		5 40/200	5 40/200	5 40/200	5 40/200	

The accuracy of the solution can also be evaluated in terms of the vertical and horizontal stresses on the remote vertical boundary. It can be shown that the vertical stresses along this boundary, determined from the finite-element analyses, are on average within 4 per cent of the equivalent overburden stresses expressed in terms of the depth below surface and the specific weight of the rock. It can further be shown that the horizontal stresses determined from the finite-element analyses are on average within 2 per cent of the horizontal stresses specified as primitive proportions of the equivalent overburden stresses.

PRESENTATION OF RESULTS

The results of the finite-element analyses were interpreted in terms of vector plots of the principal stresses. Typical examples are shown in Figures 1 and 2, in which the zones of combined tension and compression are shown hatched. Figure 1 represents a vector plot of the stresses for analysis EA2, in which the zones of biaxial compression and combined tension and compression shown are typical for an elastic medium. Figure 2 represents a vector plot of the stresses for analysis JA2, in which part failure of the discontinuities, deslimed-tailings backfill support, and a lateral-to-vertical field stress ratio of 0,25 were simulated. The relative absence of significant tensile stresses and the significant sub-horizontal compressions in the nether hangingwall are aspects typical of this case, which can be observed in Figure 2. Other aspects of the various analyses carried out are summarized in the next section, in which the findings are enumerated.

FINDINGS

The stress and load-displacement characteristics of the rockmass depend on the elastic or partly failed status of the rockmass provided for in the numerical analysis. The stress characteristics as affected by each of the parameters considered are presented separately for the analyses in which the rockmass was assumed to be elastic and in which it was allowed to fail. The two sets of characteristics are then compared for each parameter. The load–displacement characteristics are presented in conclusion.

Stress Characteristics

Discontinuity Strength—Elastic Analysis

It can be demonstrated from the plots of stress vectors that the elastic analyses for all the parameter values considered are characterized by the following.

(a) Double-lobed zones of biaxial tensile (sub-horizontal) and compressive (sub-vertical) stresses above and below the stope. Narrow zones of biaxial tensile stress occur in the nether hangingwall and footwall of the stope, depending upon the magnitude of the support reaction.

(b) Arching of the global hangingwall and footwall across the span of stope, which is associated with very high shearing stresses over the face abutments.

(c) Non-vertical and non-horizontal principal directions in general, which are associated with the arching action and abutment shears referred to.

(d) Considerable total stored shear–strain energy.

Discontinuity Strength—Non-elastic Analysis

It can be similarly demonstrated that the analyses for partly failed rock are characterized as follows.

(i) The absence of extensive zones of uniaxial or biaxial tension, except in cases of relatively small support reaction and field stress ratio. Sub-horizontal compressive stresses of significant magnitude and extent occur in the nether hangingwall and footwall.

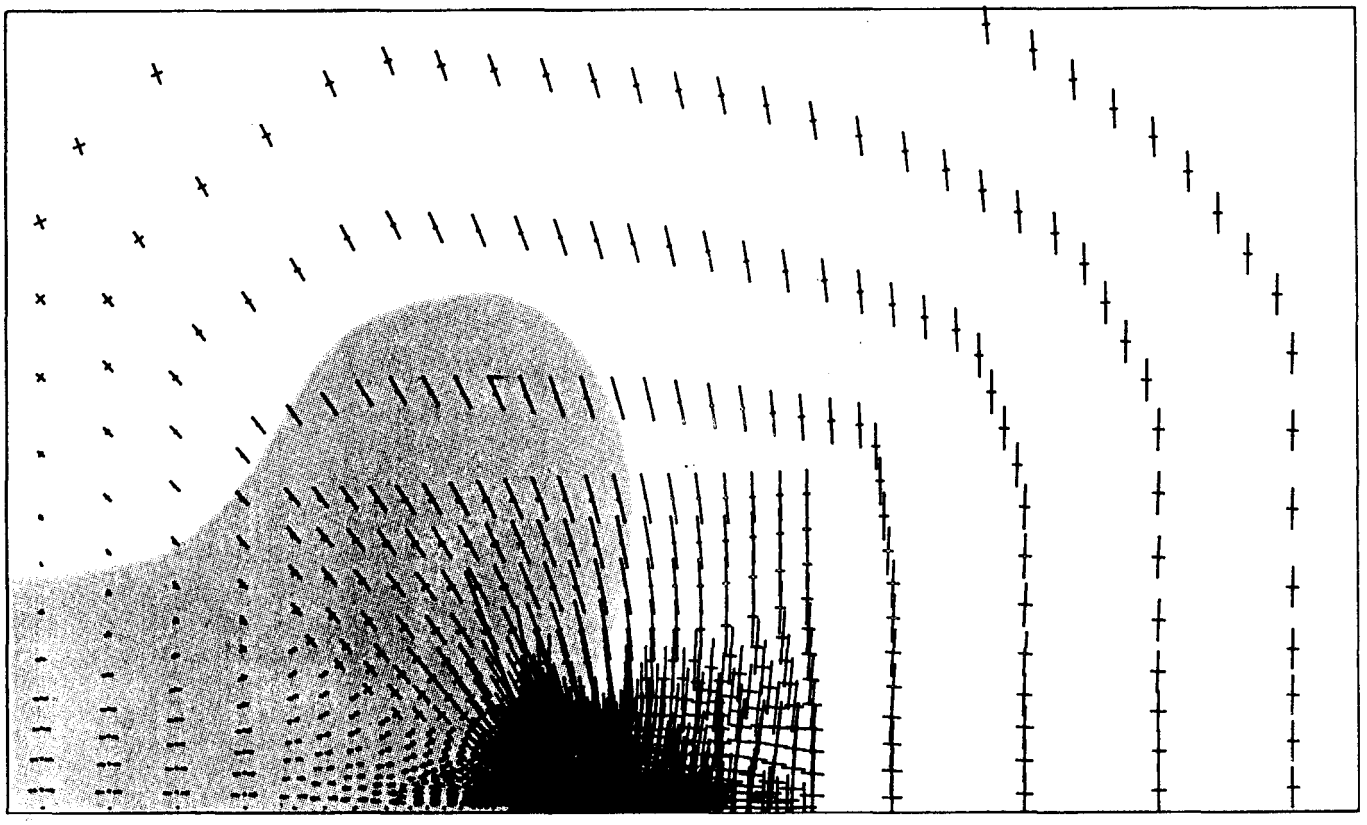

Figure 1—Vector plot of principal stresses for analysis EA2
(Combined tensions and compression zone hatched, otherwise biaxial compression)

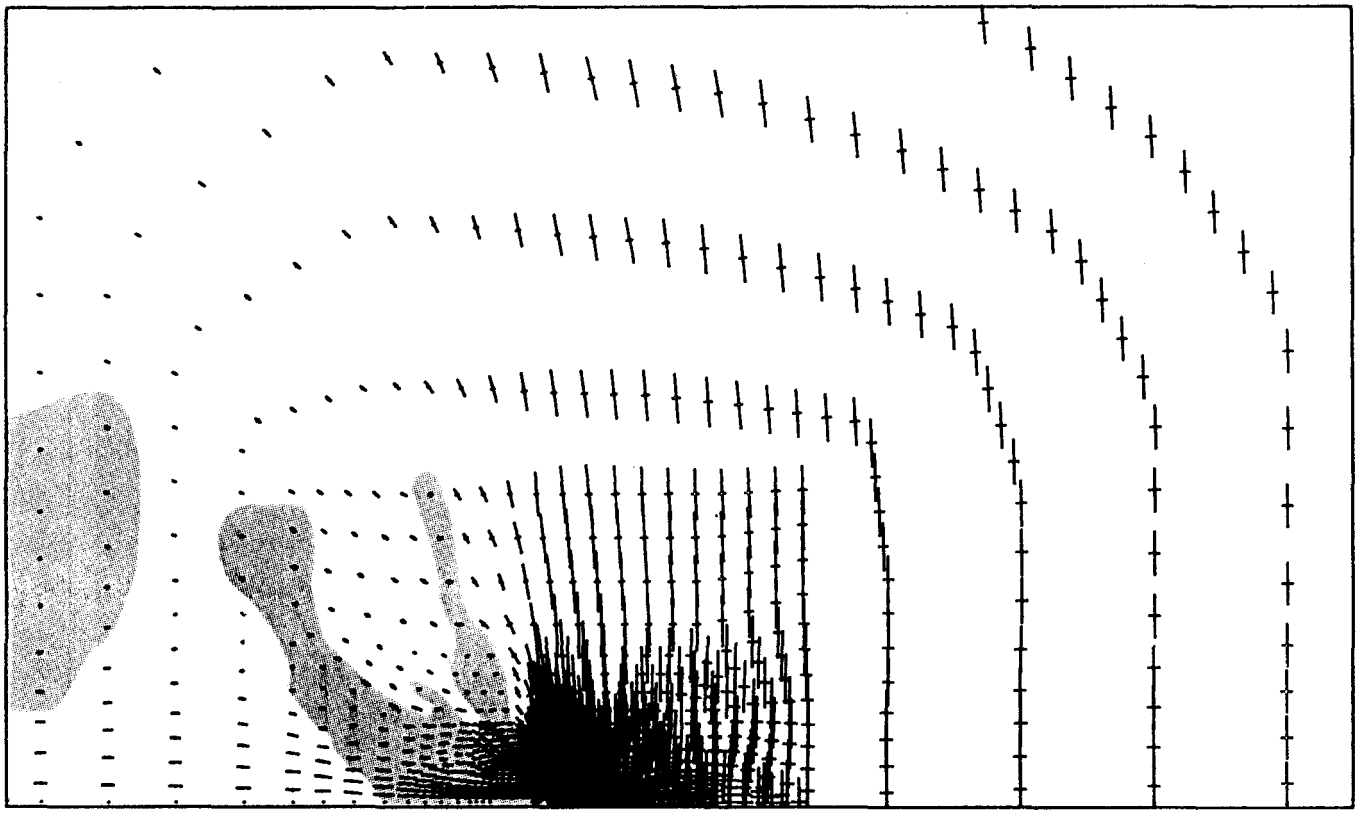

Figure 2—Vector plot of principal stresses for analysis JA2
(Combined tensions and compression zone hatched, otherwise biaxial compression)

(ii) The global hangingwall bearing directly across the stope in the vertical direction, except in the cases of relatively small support reaction. This effect is masked by a relatively large field stress ratio. A narrow, finger-like zone of significant vertical extent rises from the face over the stope at a dip angle of approximately 70 degrees in which the vertical stress tends to be slightly tensile. Variation in the maximum principal direction along any horizon is subject to contra-rotation about the horizontal at the centre of this zone.

(iii) Principal directions that are generally vertical and horizontal, except in the above described finger-like zone and except for relatively large field stress ratios.

(iv) Moderate overall amounts of stored shear–strain energy.

Discontinuity Strength—Comparison of Analyses

It is evident from respective comparisons between paragraphs (a) and (i), (b) and (ii), (c) and (iii), and (d) and (iv) that the stresses around a stope in elastic rock are completely different from those around a stope in which partial failure of the discontinuities occurs. The difference increases with the extent of failure on the discontinuities, showing that rock stresses, support reactions and energy release rates as a result cannot be determined reliably from solution schemes that are based on elastic analyses.

Depth of Mining—Elastic Analysis

The effects of the depth of mining on the stresses determined for elastic rock can be summarized as follows.

(a) The distributions of the stresses in terms of the extent and shape of zones of tension and compression, and in terms of the principal directions, are not affected significantly by the depth of mining except in the case of stiff fills as referred to below.

(b) The magnitudes of the stresses are proportionately larger for greater depths of mining, except for the effect of fill stiffness.

(c) Relatively stiff fills reduce the extent of tensile zones and increase the major principal stresses (sub-vertical) to an increasing extent with mining span.

(d) Arching of the hangingwall and footwall, and shearing over the face abutments, are not affected as such by the depth of mining. However, the magnitudes of the relevant stresses are directly proportional to the depth of mining.

Depth of Mining—Non-elastic Analysis

The effects of the depth of mining on the stresses determined for rock in which the discontinuities are subject to failure can be summarized as follows.

(i) The distributions of the stresses are, as for the elastic analysis, not significantly affected by the depth of mining, except in the case of stiff fills.

(ii) Except for the specific aspects referred to in paragraph (iv) following, and except for stiff fills, the magnitudes of the stresses are disproportionately larger for greater depths of mining owing to an increase in the extent of discontinuity failure with depth.

(iii) Relatively stiff fills increase the major principal stresses (sub-vertical) over most of the stope span. Owing to a reduced shear stiffness associated with discontinuity failure, this effect is more marked in partly failed than in elastic rock.

(iv) Horizontal clamping of the nether hangingwall, and direct bearing of the global hangingwall onto the footwall in the vertical direction, are not affected as such by the depth of mining.

Depth of Mining—Comparison of Analyses

It is evident from respective comparisons of paragraphs (a) and (i), (b) and (ii), (c) and (iii), and (d) and (iv) that the depth of mining does not affect the stress characteristics differently in the elastic and non-elastic analyses.

Mining Span—Elastic Analysis

The effects of the mining span on the stresses determined for elastic rock can be summarized as follows.

(a) The distributions of the stresses in terms of the extents and shapes of the various zones of tension and compression, the principal directions, and the magnitudes of the stresses are not significantly affected by the mining span, except in the cases of relatively small support reactions as referred to below.

(b) Arching of the hangingwall and footwall, and shearing over the face abutments, are not affected as such by the mining span, except in the cases of small support reactions.

(c) In these latter instances, the zones of tension are very much larger in vertical extent and the principal stresses are larger for larger mining spans.

Mining Span—Non-elastic Analysis

The effects of the mining span on the stresses determined for rock subject to failure of the discontinuities can he summarized as follows.

(i) As for the elastic analysis, the distributions of the stresses are not significantly affected by the mining span, except as affected in conjunction with support reaction as referred to below.

(ii) Horizontal clamping of the nether hangingwall and direct vertical bearing of the global hangingwall onto the footwall are not affected as such by the mining span except as referred to as follows by support reaction.

(iii) In situations of relatively small support reaction, horizontal clamping in the nether hangingwall is very much larger for larger mining spans. The major principal stresses (sub-vertical) are, however, independent of the mining span under these conditions. Conversely, in instances of increased fill stiffness and support reaction, horizontal clamping is independent of the mining span, and the sub-vertical principal stresses are very much larger for larger mining spans. The principal directions are reversed for small, compared with substantial, support reaction. The comparative magnitudes of the principal stresses are, however, not very different.

Mining Span—Comparison of the Analyses

It is evident from respective comparisons of paragraphs (a) and (i), (b) and (ii), and (c) and (iii) that mining span does not significantly affect the stress characteristics in the elastic or non-elastic analyses.

Field Stress Ratio—Elastic Analysis

The effects of the lateral:vertical field stress ratio on the stresses determined for elastic rock can be summarized as follows:

(a) The distributions of the stresses in terms of the extents and shapes of the various zones of tension and compression are significantly affected by the field stress ratio. An increase in the ratio reduces the extent of the tension zones in all directions over the mined-out areas.
(b) Arching of the hangingwall and footwall is affected in that an increase in the field stress ratio is accompanied by a reduction in the height to which the arch rises over the stope. The horizontal tensile stresses in the nether hangingwall are not significantly affected by an increase in field stress ratio.

Field Stress Ratio—Non-elastic Analysis

The effects of the field stress ratio on the stresses determined for rock subject to failure of the discontinuities can be summarized as follows:

(i) The distributions of the stresses in terms of the extents and shapes of the various zones of tension and compression are not significantly affected by the field stress ratio. The position of the finger-like zone in which the variation in the maximum principal direction about the horizontal is subject to contra-rotation is displaced to some extent further back from the face by an increase in the field stress ratio. Compressions in the super hangingwall are increased by larger field stress ratios.
(ii) Horizontal clamping of the nether hangingwall and direct vertical bearing of the global hangingwall onto the footwall are not affected significantly by the field stress ratio. The failed rock in the immediate vicinity of the stope and in the detached stratum in the nether hangingwall are shielded in principle by the super hangingwall from the effects of mining depth, span, and field stress ratio.

Field Stress Ratio—Comparison of Analyses

It is evident from respective comparisons of the aspects presented in paragraphs (a) and (i), and (b) and (ii) that the effects of the field stress ratio on various stress-related aspects are completely different in the elastic and non-elastic analyses. Therefore, aspects of mine design that are related to field stress ratio cannot be reliably evaluated by means of elastic analyses.

Support Stiffness

The effects of support stiffness on the stress characteristics have already been referred to but, for convenience, are summarized again as follows.

- The occurrence of vertical tensile stresses in the nether hangingwall of elastic or non-elastic media depends upon the support stiffness. If the support is relatively stiff or increases rapidly in stiffness on convergence, the tensile stresses will be reduced or completely obviated.
- In rock in which the discontinuities are subject to failure, the stiffness of the support not only obviates the tensile stresses, but enhances the extent to which the rock above the stope bears directly onto that below the stope.
- Increased fill stiffness has the effect in elastic analyses of reducing the effects of mining span on the stresses.
- In addition to giving rise to greater vertical stresses over the stopes in rock in which the discontinuities are subject to failure, increased fill stiffness results in a reduction in the horizontal clamping stresses in the nether hangingwall to the extent that these become independent of the mining span.

Load-displacement Characteristics

The load-displacement characteristics of the rock surrounding a stope in an intact elastic medium are completely different from those in a non-elastic discontinuum. The magnitude of the difference depends on the extent to which failure occurs on the discontinuities in characteristic zones around the stope, as discussed earlier.

Joints in natural rock are discontinuous on the scale of a real mine. A plane of weakness consists of unconnected sections interspaced with rock bridges. The degree of continuity, and the strength of the unconnected sections and the rock bridges, determine the extent to which failure develops on planes of weakness in conjunction with the depth and span of mining and the field stress ratio.

The rock bridges take load in preference to stope support and, depending on the depth and span of mining and the field stress ratio, may render the rockmass self-supporting; that is, the bridges may be subject to a condition of terminating failure, depending on the overall strength of the planes of weakness. Alternatively, the overall strength of the planes of weakness may be of such low overall value that the rock bridges fail in a non-terminating manner and, as a result, do not render the rockmass self-supporting. Under such conditions, the rockmass is in a state of unstable equilibrium unless the stope is actively supported or substantially converged.

The way in which the load-displacement characteristics of the rockmass are affected by joint strength, depth and span of mining, field stress ratio, and type of stope support is illustrated in Tables VII and IX in terms of stope closure and in Tables VIII and X in terms of rock-fill contact load at 5 m from the face and in the back area. These tables are laid out along the lines of the schematic arrangement of the various parameters given in Table I. As shown in Tables III to VI, the conventional support was assumed to exert a constant pressure of 300 kPa on the hangingwalls, and footwalls of the stope. The backfills were assumed to be subject to uniaxial strain paths in terms of which the generated support pressure increases exponentially with convergence. The joint strengths for the non-elastic medium were chosen so that the rockmass is self-supporting in the first case and not in the second, as represented by the middle and bottom entries in Tables VII to X respectively. The entire excavation was assumed to be mined and supported in a single step.

It is evident from the relative magnitude of stope closure in Table VII that the flexibility of the rockmass is the lowest when assumed to be an intact elastic medium. The flexibility of the rockmass increases with a decrease in joint strength for all proportions of depth:span, field stress ratio, and type of stope support. The flexibility does not increase with an increase in depth, but it does increase with span. The greater rockmass flexibility associated with a reduction in joint strength is masked in the cases representing stiffer support and longer stope spans. This is compatible with the postulated behaviour of a discontinuous rockmass.

Table IX

Hangingwall closures (mm) at 5,0 m from face and in back area, determined from finite-element analyses for various field stress ratios

Type of material	Condition of discontinuity bridges	Type of stope support												Depth:span
		Conventional matpacks and pipesticks						Deslimed tailings backfill						
Elastic continuum	Intact	32	63	32	62	32	62	32	62	32	62	32	62	2000:80
		–	–	71	176	–	–	–	–	49	109	–	–	2000:400
		–	–	64	125	–	–	–	–	61	114	–	–	4000:80
		144	360	142	354	140	350	75	147	75	147	74	145	4000:400
	Failed partly	111	170	72	107	57	95	84	117	69	94	57	87	2000:80
		246	557	159	402	117	324	92	138	87	130	76	122	2000:400
		237	375	147	228	114	196	120	158	108	140	98	130	4000:80
		501	1213	329	740	217	587	128	156	123	151	114	156	4000:400
Non-elastic discontinuum	Failing continually	No analyses attempted												– – – –
	Failed completely	127	221	80	143	54	106	86	125	72	100	56	88	2000:80
		265	559	235	486	183	380	94	140	87	133	80	124	2000:400
		255	441	156	255	108	200	123	162	110	142	101	130	4000:80
		823	1810	486	1061	373	794	130	168	123	157	120	151	4000:400
Distance from face, m Stress ratio, K		5 40/200 0,1		4 40/200 0,25		5 40/200 0,50		5 40/200 0,1		5 40/200 0,25		5 40/200 0,50		

Table X

Rock-fill contact loads (m head of rock) at 5,0 m from face and in back area, determined from finite-element analyses for various field stress ratios

Type of material	Condition of discontinuity bridges	Type of stope support												Depth:span
		Conventional matpacks and pipesticks						Deslimed tailings backfill						
Elastic continuum	Intact	12	12	12	12	12	12	3	19	3	18	3	18	2000:80
		–	–	12	12	–	–	–	–	4	387	–	–	2000:400
		–	–	12	12	–	–	–	–	12	491	–	–	4000:80
		12	12	12	12	12	12	57	2034	54	1722	50	1677	4000:400
	Failed partly	12	12	12	12	12	12	81	549	27	193	3	122	2000:80
		12	12	12	12	12	12	96	1131	110	894	36	669	2000:400
		12	12	12	12	12	12	562	2132	395	1166	143	880	4000:80
		12	12	12	12	12	12	791	3163	604	2554	381	1969	4000:400
Non-elastic discontinuum	Failing continually	No analyses attempted												– – – –
	Failed completely	12	12	12	12	12	12	114	730	35	250	0	131	2000:80
		12	12	12	12	12	12	164	1200	110	953	69	697	2000:400
		12	12	12	12	12	12	608	2404	447	1262	22	871	4000:80
		12	12	12	12	12	12	850	3250	603	2605	632	1987	4000:400
Distance from face, m Stress ratio, K		5 40/200 0,1		5 40/200 0,25		5 40/200 0,50		5 40/200 0,1		5 40/200 0,25		5 40/200 0,50		

It can be seen from Table IX that the field stress ratio has a very significant effect on the flexibility of the rockmass. For small ratios, the flexibility of the rockmass is the largest, and the concomitant horizontal clamping potential of the nether hangingwall, particularly in the vicinity of the face, is the smallest. All of these conclusions are confirmed by the indirect effect of the rockmass flexibility on the rock-fill contact loads, as given in Tables VIII and X.

It can be said as an overall conclusion that the extent to which the support is loaded behind the face, and the rate at which it is loaded, are completely different in intact elastic media compared with media in which failure is allowed on the joints. Therefore, the performance of support in a real stope surrounded by failed material cannot be evaluated by means of solution schemes that are based on elastic analyses.

SALIENT MINE PLANNING AND DESIGN IMPLICATIONS

The integrity of a stope depends primarily on the horizontal clamping stresses in the nether hangingwall and footwall, the continuity of the support as it affects the shake-out potential of the adjoining rock walls, the stability of the support in terms of developed reactions, and the stability of the face as affected by abutment stresses. The traditional approach in the design of the integrity of stopes has largely been to increase the capacity of the support and to reduce the rock stresses and the associated seismicity. This approach is irrevocably coupled with everincreasing support costs and is not feasible for mining at greater depths. It has been developed largely on an understanding of the behaviour of the rock as an elastic medium and, as such, has served the industry well over the past three decades. Continuously increasing mining costs and safety standards will increasingly require that the design of stope support and the underlying understanding of the behaviour of the rockmass should be refined. This will require more accurate modelling of the rock as a medium in which failure of the material and the discontinuities is allowed to occur.

The findings of the parametric analyses reported here give some indication of the sophistications that will have to be incorporated in support designs in future. They indicate, in principle, that elastic analyses are generally not sufficiently reliable for the modelling of the complex behaviour of the rock surrounding a stope in which discontinuities may fail to some extent. The characteristics of partially failed rock are so different from those of elastic rock that the design rules of thumb and the experiential judgement developed on the basis of elastic analyses are also not reliable. The implications of the effect of the modelling basis on design decisions can be illustrated in terms of horizontal clamping in the nether hangingwall.

Although the level of seismic activity increases with depth, the safety and stability of the working area in a backfilled stope will not be adversely affected at greater depth owing to the clamping effect in the nether hangingwall and the continuity of the backfill. Although horizontal clamping is not significantly affected by the depth of mining, it will be sufficient to prevent shake-out in conjunction with the continuity of the backfill. However, a conventionally supported stope, by comparison, is likely to be subject to greater shake-out potential and greater instability at greater depth.

The horizontal clamping stresses in the nether hangingwall increase with an increase in the span of conventionally supported stopes, and remain relatively unaffected by changes in span if the stope is filled with a relatively compressible fill. The safety and stability of the working area in such backfilled stopes should therefore not vary with span. By comparison, the integrity of a conventionally supported stope is likely to decrease with an increase in span owing to an increase in shake-out potential associated with increased levels of seismicity.

Horizontal clamping of the nether hangingwall is also not affected significantly by the field stress ratio. The integrity of a stope is therefore not affected as such by the field stress ratio or by differences in the field stress ratio in the different mining districts into which the face may be advanced. The type of support may, however, have a significant effect on the integrity of the stope similar to that indicated in the preceding paragraphs for backfill and conventional support respectively.

An increase in support stiffness results in a decrease in the horizontal clamping stresses in the nether hangingwall. Notwithstanding the fact that relatively soft fills will provide adequate support irrespective of depth, span, and field stress ratio, an increase in fill stiffness will improve the safety and stability of a stope. The increased support reaction and the resulting reduction in the level of seismic activity provided by a relatively stiff fill will outweigh the accompanying adverse effect of reduced clamping stresses. It must be emphasized, however, that a relatively compressible fill like deslimed tailings will, owing to its continuity, provide an adequate supporting medium.

VERIFICATION OF SIMULATED BEHAVIOUR OF PARTLY FAILED ROCK

The behavioural characteristics of non-elastic rock referred to have been verified in the research work of others. Some of the key examples in this regard are described here briefly.

Coulthard and Dutton[6] simulated the subsidence induced by the extraction of single panels of coal with continuum and distinct element solution schemes, and showed that parameter values determined from the back-fitting of elastically calculated displacements to field observed displacements do not represent the fundamental behaviour of rock that is subject to failure. Such values for the material parameters do not enable the displacements for different mining configurations (for example, stope span, and width) to be calculated reliably. The accuracy with which observed subsidence profiles can be simulated depends on the properties of the intact rock and the discontinuities, and on the structure of the rock (that is, discontinuities) considered.

Squelch[7] measured the horizontal stresses in the first 2,5 m of hangingwall rock within 4 m of the face of backfilled and conventional stopes. He found in backfilled stopes that both the major and the minor principal horizontal stresses were compressive and increased in magnitude into the hangingwall. In conventional stopes, the major principal horizontal stress was compressive and increased in magnitude into the hangingwall, and the minor principal horizontal stress was tensile.

Gürtunca and Adams[8] compared *in situ* measurements of stress and displacement with values for these quantities determined from three different numerical simulations. In the first instance, the rock was assumed to be elastic, homogeneous, and isotropic; in the second case, joint failure was allowed; and, in the third case, horizontal layers of shale were included. They found that stresses and displacements, determined from analyses in which the inelastic effects of non-homogeneities, discontinuity failure, and dilation were allowed, differed very greatly from determinations of these quantities from analyses in which the rock was assumed to be elastic, homogeneous, and isotropic. Only when they allowed for the effects of non-homogeneities and joints could the field observed stresses and displacements be approached. Gürtunca and Adams recommended that the effects of joints should not be ignored because of their significant influence on stope convergence.

However, their proposal that an 'equivalent modulus' approach be followed to allow for the effect of joints is incorrect insofar as it would not represent the fundamental difference in constitutive behaviour between an intact elastic continuum and one in which failure is allowed to occur. An equivalent modulus for a particular mining configuration cannot be applied reliably to subsequent configurations in which stope advances are modelled, because it is not uniform across the model and because it changes as the displacements associated with failure increase.

Gürtunca and Adams[9] measured the *in situ* performance of backfill materials and assessed their effectiveness in reducing rockburst damage. They found that backfill provides significant regional and local support. The closure rates and seismically induced rockburst damage in backfilled stopes were significantly reduced compared with conventional stopes, provided the backfill was properly placed.

In analytical examinations of the effect of loading history on the generation of horizontal stress in the nether hangingwall, Kuijpers and Napier[10] found that the build-up of horizontal stresses in the stope skin was essentially related to the number, and not to the size, of the mining steps. Notwithstanding, the horizontal stresses referred to are primarily due to the failure on discontinuities in the rock, as demonstrated here.

The present paper was first submitted for publication in May 1989 and has not been changed since. The findings of the various authors referred to, which post-date this study with one exception, evidently confirm all the postulates advanced. This leaves no further doubt about the limited usefulness of elastic theory with regard to natural rock, which, with its innate weaknesses and idiosyncrasies, is sufficiently heavily stressed in deep-level gold mines to be subject to failure. The safety and stability of the working place in gold mines will be far better provided for in future on the basis of this understanding.

ACKNOWLEDGEMENTS

The permission of Vaal Reefs Exploration & Mining Company Limited to publish this paper is gratefully acknowledged.

REFERENCES

1. KIRSTEN, H.A.D., and STACEY, T.R. Backfill support mechanisms in stopes with low convergence, *Proceedings Symposium on Backfill in South African Mines*. Johannesburg, South African Institute of Mining and Metallurgy and Association of Mine Managers of South Africa, 1988. pp. 137–151.
2. DESAI, C.S., and SIRIWARDANE, H.J. *Constitutive laws for engineering material with emphasis on geological materials*. New Jersey (USA), Prentice-Hall Inc., 1983.
3. KIRSTEN, H.A.D., and STACEY, T.R. Stress-displacement behaviour of the fractured rock around a deep tabular stope of limited span, *J. S. Afr. Inst. Min. Metall.*, vol. 89, no. 2. Feb. 1989. pp. 47–58.
4. STACEY, T.R. Stability of rock slopes in mining and civil engineering situations. University of Pretoria, Ph.D. thesis, 1973. 217 pp.
5. DIERING, J.A.C. Mining simulation of tabular excavations using finite elements. *Proceedings 4th International Conference on Numerical Methods in Geomechanics*. Edmonton (Canada), 1982. vol. 2, pp. 545–550.
6. COULTHARD, M.A., and DUTTON, A.J. Numerical modelling of subsidence induced by underground coal mining. *Key Questions in rock mechanics*. Cundall *et al.* (eds.). Rotterdam, Balkema, 1988.
7. SQUELCH, A.P. Horizontal stresses in the face area hangingwall of backfilled and conventional stopes at Vaal Reefs. Johannesburg, Chamber of Mines Research Organization, Internal Note, no. R16/90. 1990.
8. GÜRTUNCA, R.G., and ADAMS, D.J. Determination of the *in situ* modulus of the rockmass by the use of backfill measurements. *J. S. Afr. Inst. Min. Metall.*, vol. 91, no. 3. Mar 1991. pp. 81–88.
9. GÜRTUNCA, R.G., and ADAMS, D.J. A rock-engineering monitoring programme at West Driefontein gold mine, *J. S. Afr. Inst. Min. Metall.*, vol. 91, no. 12. Dec. 1991. pp. 423–433.
10. KUIJPERS, J.S., and NAPIER, J.A.L. The effect of loading history on stress generation due to inelastic deformations around deep-level tabular stopes, *J. S. Afr. Inst. Min. Metall.*, vol. 91, no. 6. Jun. 1991. pp. 183–194.